

# *Evaluation of CHIRPS rainfall estimates over Iran*

Article

Accepted Version

Saeidizand, R., Sabetghadam, S., Tarnavsky, E. and Pierleoni, A. (2018) Evaluation of CHIRPS rainfall estimates over Iran. Quarterly Journal of the Royal Meteorological Society, 144 (S1). pp. 282-291. ISSN 1477-870X doi: <https://doi.org/10.1002/qj.3342> Available at <https://centaur.reading.ac.uk/78251/>

It is advisable to refer to the publisher's version if you intend to cite from the work. See [Guidance on citing](#).

To link to this article DOI: <http://dx.doi.org/10.1002/qj.3342>

Publisher: Royal Meteorological Society

All outputs in CentAUR are protected by Intellectual Property Rights law, including copyright law. Copyright and IPR is retained by the creators or other copyright holders. Terms and conditions for use of this material are defined in the [End User Agreement](#).

[www.reading.ac.uk/centaur](http://www.reading.ac.uk/centaur)

**CentAUR**

Central Archive at the University of Reading

Reading's research outputs online

## Abstract

The Climate Hazards Group Infrared Precipitation with Station data (CHIRPS) dataset, first released in 2014, is a high-resolution blended rainfall product with quasi-global coverage that has not been previously evaluated over Iran. Here, we assess the performance of the CHIRPS rainfall estimates against ground-based rainfall observations across Iran over the time period from 2005 to 2014 inclusive. Results show that CHIRPS' performance is better over areas and during the months of predominantly convective precipitation with highest correlations in the southern coastal lowlands characterized by heavy rains from convective origin. Correlations are stronger with variables such as altitude, particularly alongside coastal regions in the north and south, where surface water produces more moisture in the atmosphere. Results of pairwise comparison statistics and categorical skill scores reveal the influence of altitude and precipitation amount, while categorical skill metrics vary more with changes in precipitation amount than with latitudinal or longitudinal changes.

**Keywords:** CHIRPS, rainfall, statistical evaluation.

## 1. Introduction

Water has been an inherently key resource in the social and industrial success of communities globally. Reliable, continuous, and spatially explicit surface observation of rainfall is needed to monitor and anticipate extreme events in order to mitigate their consequences. Ground-based rainfall observations can have discontinuous records over time and space, thus providing a poor overview of real rainfall. Therefore, the scientific and practitioner communities have relied on alternative data sources to estimate rainfall for a variety of applications. Satellite-derived rainfall products provide a spatially-contiguous alternative to sparse ground observations; however, such products rely on ground observations for calibration, retrieval, error/bias correction, and/or validation. Continuous improvements in the development of skillful rainfall products that make

This article has been accepted for publication and undergone full peer review but has not been through the copyediting, typesetting, pagination and proofreading process, which may lead to differences between this version and the Version of Record. Please cite this article as doi: 10.1002/qj.3342

optimal use of both satellite and ground observations have enabled their wide use for a range of applications such as drought and flood early warning, food security monitoring, and hydrological analyses.

Some rainfall products, such as the Global Precipitation Climatology Center (GPCC) dataset, are based only on *in situ* observations and include data as early as 1901 to present (Rudolf et al., 2003). Although the GPCC data provide global coverage, it has been achieved through spatial interpolation of ground-based observations and their horizontal resolution is fairly coarse at 0.5°, 1°, and 2.5° latitude-longitude for the monthly product (Schneider et al., 2014). On the other hand, satellite-only and blended products are available from the Tropical Rainfall Measuring Mission (TRMM) with records starting in 1997/98 at 0.25° horizontal resolution and at 3-hourly, daily, and monthly time steps (Kummerow et al., 1998; Huffman et al., 2007). After years of successful operation TRMM was officially terminated in 2015 and is superseded by the Global Precipitation Measurement (GPM) mission. The first combined TRMM and GPM time series are expected in 2018.

Blended datasets benefit from both *in situ* observations and satellite records and their blending algorithms are designed to support rainfall monitoring under different climatic regimes. CHIRPS was released in 2014 by the Climate Hazards Group at the University of California, Santa Barbara (UCSB) (Funk et al., 2014). CHIRPS provides higher horizontal resolution than other operational datasets at 0.05° latitude-longitude grid and quasi-global coverage (50°N-50°S, 180°W-180°E) with daily, pentadal, and monthly precipitation datasets (Funk et al., 2014). In areas of substantial decrease in the number of observations over the last decade such as Africa and southwest Asia (Funk et al., 2014), alternative sources of information on rainfall such as CHIRPS, have been widely adopted (Katsanos et al., 2016). Previous studies have shown that CHIRPS rainfall estimates closely approximate GPCC records from 1981 to 2010 (Katsanos et al., 2016) and in East Africa (Funk et al., 2013). Shukla et al. (2014) used CHIRPS in East Africa to evaluate soil moisture forecasts in the rainy, crop growing season (March-April-May). Toté et al. (2014) reported that the skill of CHIRPS for flood and drought monitoring applications in Mozambique exceeds that of other routinely used rainfall products.

Different evaluations of satellite rainfall estimates have been carried out over Iran (e.g. Javanmard et al., 2010; Katiraie-Boroujerdy et al., 2013; Moazami et al., 2016; Alijanian et al., 2017). The evaluation of different satellite rainfall estimates reveals that the results vary in

different areas (Katiraie-Boroujerdy et al., 2013). However, Moazami et al. (2016) focused on a comprehensive evaluation of four satellite rainfall estimates over Iran, including PERSIANN, TMPA-3B42-V7, TMPA-3B42RT and CMORPH. Their results show that in the most cases the underestimation in rainfall is quite large at high rainfall ranges. Although different evaluations of satellite rainfall estimates have been carried out over Iran, there have been no attempts to assess the performance of CHIRPS. Since the application of monthly rainfall data in the management of water supply is very interesting in local applications, the aim of this study is to address the following questions: 1) To what extent does CHIRPS correspond to ground-observed rainfall in Iran, 2) Is the performance of CHIRPS different over time, 3) Is the reliability of CHIRPS homogeneous across different regions, and 4) Does rainfall amount affect the correlation between CHIRPS and ground observations? If so, what are the characteristics and trend of this relationship.

## 2. Study Area

Iran's territory (approx. 1.6 million km<sup>2</sup>) extends between 25°-40°N, and is characterized by a large variety of climates (see Figure 1 in Pourvahidi and Ozdeniz, 2013), therefore precipitation has a high spatial and temporal variability. There are many studies on the spatio-temporal variability in seasonal precipitation over the country (e.g. Tabari and Talaee, 2011; Some'e et al., 2012; Moazami et al. 2016). Temporally, most of the precipitations fall during winter and autumn, however, there are regions in the northwestern part of the country that are characterized by high precipitation also during spring (Raziei et al., 2009). Northern Iran is under the influence of westerlies and Mediterranean rainfall systems. Occasionally, Siberian air masses and maritime effects produce rains alongside the Caspian Sea. Due to the proximity of the sea and the Alborz mountain chain, rainfall events may easily occur. In central and eastern Iran, precipitation is mostly limited to Mediterranean air-masses. The western part of Iran, with the prominent role of the Zagros mountain range, is influenced by westerlies. The southern lowland area receives moist air from both the Persian Gulf and southern track of westerlies. Thus, two main mountain ranges of Iran – Zagros in the west and Alborz in the north – introduce more climatic complexity. Most of Iran falls under arid/semi-arid climate, posing a chronic risk of water crises, especially in the dry season (June-August) (Bitaraf, 2000; Motiee et al., 2001). This highlights

the importance of a skillful monitoring product for rainfall across the country, particularly in regions such as central and eastern Iran where gauge network coverage is most sparse.

### 3. Data and Methodology

#### 3.1. Rain Gauge Observations

Rain gauge observations covering the time period from 2005 to 2014 inclusive were obtained from the Iranian Meteorological Organization. The stations used in the CHIRPS satellite-gauge merging process were removed from the analysis (squares in Figure 1). After quality screening of the data from the remaining stations, a total of 68 stations were included in this evaluation (circles in Figure 1). The 6-hourly gauge records were cumulated to monthly totals for over the 2005-2014-time period taking into consideration only those months with 90% of available measurements.

*Figure 1. Locations of the stations used in the CHIRPS satellite-gauge merging process (black squares) and the 68 stations in Iran included in the study (gray circles).*

#### 3.2. CHIRPS Estimates

CHIRPS monthly rainfall estimates were obtained from <ftp://ftp.chg.ucsb.edu/pub/org/chg/products/CHIRPS-2.0/>. CHIRPS is produced at different stages, starting with satellite thermal infrared (TIR) images and applying successive adjustments as described in Funk et al. (2014) and summarized below. First, the Cold Cloud Duration (CCD) technique is applied to TIR images with a uniform threshold of 235K globally to calculate cold clouds persistence (i.e. clouds that are likely to be raining) in order to identify rainy areas. Next, a linear regression best fit analysis is carried out for CCD values and the 0.25° Tropical Rainfall Measuring Mission Multi-satellite Precipitation Analysis (TMPA) 3B42 pentadal precipitation archive from 2000 to 2013 to identify the regression model's coefficients. Values from the regression model are then divided by the mean precipitation estimates from 1981-2013 and multiplied by the same grid value of CHPclim to produce the CHIRP estimate (Funk et al., 2015b). CHPclim is a geospatial modeling approach based on moving window regressions and inverse distance weighting interpolation, that combines satellite fields, gridded physiographic indicators, and in situ climate normals (Funk et al., 2015a). In the next stage, station observations are blended. The blending procedure is a modified inverse distance weighting algorithm with several unique characteristics (Funk et al. 2015b). Stations are ranked according to their quality with national stations normally having higher ranks and automated stations usually at the bottom

of the list. For each pixel, the five closest stations to the pixel are chosen for the blending procedure (Funk et al., 2014). Figure 2 shows the contribution of Iranian stations to the CHIRPS procedure since 1981. CHIRPS products are operationally generated as preliminary and final products. Final monthly products with optimal adjustments are used in the current study.

*Figure 2. Number of stations used in the CHIRPS estimation algorithm over time (Source: <ftp://ftp.chg.ucsb.edu/pub/org/chg/products/CHIRPS-2.0/diagnostics/stations-perMonth-byCountry/pngs/Iran.073.station.count.CHIRPS-v2.0.png>).*

### **3.3. Statistical Evaluation Methods**

CHIRPS primary daily and pentadal data are adjusted using CHIRPS monthly data to produce the final records (Funk et al., 2014). Hence CHIRPS monthly data have been evaluated against monthly cumulative observation records over the 2005-2014-time period. Two groups of statistics were used in the evaluation: pairwise comparison statistics to compare the ‘skill’ of the satellite product in estimating the amount of precipitation, and categorical validation statistics to evaluate the detection efficiency of CHIRPS (Toté et al., 2015). Table 1 describes the pairwise comparison and categorical validation statistics used here, where bias expresses the bias ratio as indicated by (Toté et al., 2015). Calculating categorical skills requires a threshold for rainfall and here, this was set to 0.1 mm. Since most of Iran’s territory is in the arid/semi-arid climatic region, there is a clearly defined wet season with little precipitation in the central and eastern provinces and increasing precipitation in the north and west parts of the country. This is partly due to the orographic effect of mountain ranges such as Alborz in the north and Zagros in the west, as well as related to the proximity of the Caspian Sea in the north and the Mediterranean air masses intruding into this part of the country. Thus, we apply the statistical metrics of skill for all seasons and across the country.

## **4. Results and Discussion**

### **4.1. Overall Results**

Figure 3 shows the distribution of 651 satellite and rain gauge data pairs. For lower rainfall amounts CHIRPS tends to overestimate the gauge observations, while for heavy rainfall amounts it underestimates the gauge observations. This is a known feature of satellite-based products more generally (Qin et al., 2014) and in the case of CHIRPS, likely due to the use of TMPA 3B42 to calibrate the regression model as part of the rainfall estimation algorithm. Heavy rainfall events typically occur during winter in Iran with the heaviest rainfalls recorded for Lahijan station in the north where different orographic lifting mechanisms contribute to monthly rainfall

totals. As each lifting mechanism could result in a different cloud top temperature, the low satellite-gauge correlation for higher rainfall amounts could be explained by this complexity. False alarm ration (FAR), evaluated over the whole period, is higher for low rainfall totals with a value of 0.28, likely due to cloudy but dry days mistaken by satellite imagery as rainy, especially in arid and semi-arid regions. This could also due to sub-cloud evaporation of the rain drops. Moazami et al., (2013) reported this specific problem in the semi-arid region of Iran, where raindrop tend to evaporate before they reach the surface with a consequent high FAR. Moreover, the presence of cirrus clouds results in false alarms and cold surfaces detected as rainy areas in TRMM's passive microwave imagery, particularly in the highlands. Relative mean absolute error (RMAE) and bias values were also examined for different rainfall categories. In high rainfall amounts there is underestimation and for low rainfall amounts there is overestimation. On both sides of the ideal value for bias (1), underestimation and overestimation might seem of the same magnitude, but RMAE shows more deviation from observations on the side of underestimation.

*Figure 3. Linear regression analysis of CHIRPS estimates and rain-gauge observations (in mm/year) across Iran over the 2005-2014 time period. The dashed line represents the 1:1 relationship between CHIRPS and rain gauge data pairs ( $y = 0.698x + 16.1$   $R^2 = 0.368$ ).*

#### 4.2. Seasonal Evaluation

Figure 4 shows the seasonal comparisons over Iran. Characteristics of each dataset including median, skewness, dispersion and extreme rainfall are depicted for each season. Statistical evaluation shows that the highest correlations are for the Spring when convection is the common lifting mechanism, especially in areas of moist air and decreasing frontal rains.

*Figure 4. CHIRPS seasonal evaluation over Iran (2005-2014). The box plot advocated here is a graphical summary of a given dataset, which includes the median, the interquartile range (shown by the boxes) and the rainfall extremes.*

Table 2 summarizes the results for all seasons with the highest correlation and RMAE and FAR values with the least deviation from the perfect score values in the spring. Bias is closest to the perfect score in autumn. In Iran summer is the dry season, except for rains in the Caspian littoral and the highlands in the northwest. However, there is a fairly good correlation, significant at 0.01 level during summer. Even though bias values are similar and closest to the perfect score of 1 for summer and autumn, the correlation, RMAE, and FAR are closest to their respective perfect scores in spring, indicating that the gauge-satellite agreement is most robust for the spring. The



highest FAR in summer can be at least in part explained by the high chance of non-raining clouds, which may produce brief localized showers.

Most of the annual rainfall over Iran is received in the winter. However, in the Caspian littoral most rainfall was received in autumn over the years considered in this study. In autumn, the orographic lifting mechanism causes upper-level disturbances, surface disturbances, and a combination of both known as westerly disturbances (Alijani and Harman, 1985). These mechanisms likely explain the lower correlation during autumn. The high FAR for autumn is due to spatial averaging over Iran's diverse climates, which includes arid and semi-arid regions that at the beginning of autumn are still under summer-like climatic regime. It is worth noting that all validation statistics, except for FAR, were poorest for winter (see Table 2). The highest bias values in winter are likely due to the high number of cloudy days without rainfall, i.e. warmer stratiform clouds. RMAE is also highest in the Winter. FAR is lowest in winter due to winter being the wettest season and the evaluation being carried out at the monthly time step. A daily step evaluation is likely to result in higher FAR values, as the bias is highest in this season. Other statistics like the probability of detection (POD) could have been adopted, but don't produce significant results. POD indicates the fraction of the observed events that correctly forecast and in the current study, seasonal POD values are uniformly around the perfect score of 1.

#### **4.3. Monthly Evaluation**

The results from the monthly evaluation of CHIRPS against gauge observations for the 10-year period over Iran are shown in Figure 5. During the wet seasons, correlations are typically low. The lowest correlation is observed in January; however, RMAE is highest in January likely due to the high number of cloudy but dry days. Spring months are characterized by better agreement between CHIRPS estimates and gauge observations in terms of correlation, bias, and RMAE, as rainfall in springtime is mostly from convective lifting mechanism, which are amenable to the CCD algorithm of CHIRPS. Correlation is highest in May. Bias is optimal in November, but also May-July, while RMAE values are closest to the perfect score of 0 in November, as well as April and May. As discussed above, FAR values are close to the perfect score of 0 in the time period between Nov and April, and this is expected due to using the monthly time step of evaluation.

*Figure 5. Monthly evaluation of CHIRPS against gauge observations over Iran for the 2005-2014 time period.*

#### 4.4. Spatial Evaluation

Figure 6 shows the distribution of correlations across Iran. In the southeast part of the country, stations are sparse and often have intermittent records. Although stations with large gaps in the records were excluded from the analysis at the preprocessing stage, at least two of the remaining stations have poor correlations. Along the Caspian Sea coast, where diverse lifting mechanisms operate, correlations are lowest for three stations. However, in the mountainous area correlations are moderate to high, despite low-cloud rainfall being usually missed by satellites, the variability of cloud-top temperatures is smaller, making it amenable to detection with the CHIRPS CCD algorithm, which uses a uniform temperature threshold.

*Figure 6. Distribution of CHIRPS-gauge correlations across Iran for the 2005-2014 time period. Circles indicate high correlations, squares -- moderate, and triangles -- low correlations (all correlations are significant at the level of 0.01).*

Figure 7a and 7b show the trends in CHIRPS-gauge correlations across Iran with latitude and altitude, respectively. Correlations vary as altitude changes and are slightly higher for higher altitudes (Figure 7a). The relationship with latitude is non-linear (Figure 7b), and not meaningful most likely due to the topography and complex orographic lifting mechanisms in the north where correlations decrease. The best fit (linear or nonlinear) has been chosen.

*Figure 7. Correlations relative to (a) altitude and (b) latitude. Solid line is the best fit regression line between correlation values and altitudes.*

Figure 8 shows the variation of CHIRPS-gauge bias values across Iran. According to both Fig. 6 and Fig. 8 CHIRPS works better for stations located in the western side of the country. Bias values and altitude are strongly related in the Caspian littoral, i.e. underestimation turns into overestimation for higher altitudes (Figure 9a-b). In this region, precipitation events from low-level clouds are difficult to detect even at higher-altitude stations, while they are easier to detect by satellite imagery. Low-level clouds tend to have higher cloud top temperatures and thus, satellite-based detection would underestimate the rainfall. In the southern lowlands, there is an inverse trend, even though, there are only a few stations in this part of the country (Figure 9c). Although rain is scarce in the southern lowlands, atmospheric water transforms from gas to liquid droplets with increasing altitude. Since it is more likely to have non-raining clouds over lowlands than in the highland regions and passive microwave instruments detect precipitation based on the ice content of the atmosphere, higher FAR values and rainfall overestimation are expected in lowland regions.

Figure 8. Distribution of CHIRPS-gauge bias values over Iran. Circles indicate overestimation, squares indicate underestimation; for both markers, the darker the color, the closer the bias value is to the perfect score of 1.

Figure 9. The changes in bias values with monthly time resolution, alongside (a) the Caspian Sea:  $R^2 = 0.5141$ , (b) the whole country:  $R^2 = 0.0662$  and (c) the southern area:  $R^2 = 0.5667$ . Dashed line is the best fit regression between bias values and altitude.

Figures 10a-c show the trends of FAR values relative to latitude, longitude and rainfall respectively. FAR values are closer to the perfect score of 0 with increasing rainfall. Therefore, CHIRPS rainfall estimates are more reliable for higher latitudes. However, in longitudinal direction the eastern part of the country exhibits poorer FAR values, mainly due to the presence of the Zagros mountain barrier, which limits the entry of westerlies to the inner part of Iranian Plateau. Atmospheric moisture is generally higher in the south than in the north; however, the atmosphere is dynamically stable there and the frequency of rainy days is smaller than in the north. Northern areas are more dynamically unstable due to the proximity of the polar frontal jet stream, whereas the south is governed by the weaker and higher extratropical jet stream. Moreover, the southern coastal region is affected by the subtropical high pressure belt.

Figure 10. Trends in FAR values relative to (a) latitude ( $y = -0.0413x + 1.6178$ ,  $R^2 = 0.7731$ ), (b) longitude ( $y = 0.0235x - 1.022$ ,  $R^2 = 0.374$ ), and (c) rainfall amount ( $y = -0.137\ln(x) + 0.959$ ,  $R^2 = 0.519$ ).

## 5. Conclusions

We evaluated monthly CHIRPS rainfall estimates against ground-based rain gauge observations over Iran for the decade from 2005 to 2014. In an overall comparison across Iran disregarding time or location, CHIRPS resulted in overestimation, despite the fact that correlation was reliable at the significance level of 0.01. However, results differ regionally and over time, particularly related to the characteristic presence of different orographic lifting mechanisms. The temporal evaluation shows that the closest CHIRPS-gauge agreement, indicated by all validation statistics, occurs in spring when convective rainfall is prevalent. Pairwise comparison statistics indicate stronger correlations with variables such as altitude, particularly alongside coastal regions in the north and south, where surface water produces more moisture in the atmosphere. In comparison to pairwise statistics, categorical measures, which are sensitive to the selected threshold for rainy days, vary more with changes in precipitation amount than with latitudinal or longitudinal changes.

## References

- Alijani B and Harman JR. 1985. Synoptic climatology of precipitation in Iran. *Annals of the Association of American Geographers*, 75(3): 404-416. DOI: 10.1111/j.1467-8306.1985.tb00075.x.
- Alijanian M, Rakhshandehroo G, Mishra, A and Dehghani M. 2017. Evaluation of satellite rainfall climatology using CMORPH, PERSIANN-CDR, PERSIANN, TRMM, MSWEP over Iran. *International Journal of Climatology*, 37(14), pp.4896-4914.
- Bitaraf H. 2000. *Protecting Water Resources in Iran*. Iranian Water and Wastewater Journal (Shahrab) No. 223.
- Funk C, Husak G, Michaelsen J, Shukla S, Hoell A, Lyon B, Hoerling MP, Liebmann B, Zhang T, Verdin J and Galu G. 2013. Attribution of 2012 and 2003-12 rainfall deficits in eastern Kenya and southern Somalia. *Bulletin of the American Meteorological Society*, 94(9): S45.
- Funk CC, Peterson PJ, Landsfeld MF, Pedreros, DH, Verdin JP, Rowland JD, Romero BE, Husak GJ, Michaelsen JC, Verdin AP and Pedreros P. 2014. A quasi-global precipitation time series for drought monitoring. *US Geological Survey Data Series*, 832(4).
- Funk C, Verdin A, Michaelsen J, Peterson P, Pedreros D, Husak G. 2015a. A global satellite-assisted precipitation climatology. *Earth System Science Data*. 1;7(2):275. DOI:10.5194/essdd-8-401-2015
- Funk C, Peterson P, Landsfeld M, Pedreros D, Verdin J, Shukla S, Husak G, Rowland J, Harrison L, Hoell A, Michaelsen J. 2015b. The climate hazards infrared precipitation with stations—a new environmental record for monitoring extremes. *Scientific data*. 8; 2:150066. DOI:10.1038/sdata.2015.66.
- Huffman GJ, Bolvin DT, Nelkin EJ, Wolff DB, Adler RF, Gu G, Hong Y, Bowman KP and Stocker EF. 2007. The TRMM multisatellite precipitation analysis (TMPA): Quasi-global, multiyear, combined-sensor precipitation estimates at fine scales. *Journal of Hydrometeorology*, 8(1): 38-55. DOI:10.1175/JHM560.1.
- Javanmard S, Yatagai A, Nodzu MI, BodaghJamali J, Kawamoto H. 2010. Comparing high-resolution gridded precipitation data with satellite rainfall estimates of TRMM\_3B42 over Iran. *Advances in Geosciences*. 17;25:119-25. DOI: 10.5194/adgeo-25-119-2010.
- Katsanos D, Retalis A and Michaelides S. 2016. Validation of a high-resolution precipitation database (CHIRPS) over Cyprus for a 30-year period. *Atmospheric Research*, 169: 459-464. DOI:10.1016/j.atmosres.2015.05.015.
- Katiraie-Boroujerdy P, Nasrollahi N, Hsu K and Sorooshian S. 2013. Evaluation of satellite-based precipitation estimation over Iran. *Journal of arid environments*, 97, 205-219.
- Kummerow C, Barnes W, Kozu T, Shiue J and Simpson J. 1998. The tropical rainfall measuring mission (TRMM) sensor package. *Journal of atmospheric and oceanic technology*, 15(3): 809-817. DOI: 10.1175/1520-0426(1998)015.
- Moazami S, Golian S, Kavianpour M and Hong Y. 2013. Comparison of PERSIANN and V7 TRMM Multi-satellite Precipitation Analysis (TMPA) products with rain gauge data over Iran. *International journal of remote sensing*, 34(22), 8156-8171. DOI: 10.1080/01431161.2013.833360.
- Moazami S, Golian S, Hong Y, Sheng C, Kavianpour MR. 2016. Comprehensive evaluation of four high-resolution satellite precipitation products under diverse climate conditions in Iran. *Hydrological Sciences Journal*. 25;61(2):420-40. DOI: 10.1080/02626667.2014.987675.

- Pourvahidi P and Ozdeniz MB. 2013. Bioclimatic analysis of Iranian climate for energy conservation and architecture. *Scientific Research and Essays*, 8(1): 6-16.
- Raziei, T., Saghafian, B., Paulo, A.A., Pereira, L.S., Bordi, I., 2009. Spatial patterns and temporal variability of drought in western Iran. *Water Resour. Manage.* 23, 439–455. DOI 10.1007/s11269-008-9282-4
- Rudolf B, Fuchs T, Schneider U and Meyer-Christoffer A. 2003. Introduction of the Global Precipitation Climatology Centre (GPCC), Deutscher Wetterdienst, Offenbach a.M.; pp. 16, available on request per email gpcc@dwd.de or by download from GPCC's Website.
- Schneider U, Becker A, Finger P, Meyer-Christoffer A, Ziese M and Rudolf B. 2014. GPCC's new land surface precipitation climatology based on quality-controlled in situ data and its role in quantifying the global water cycle. *Theoretical and Applied Climatology*, 115(1-2): 15-40. DOI: 10.1007/s00704-013-0860-x.
- Shukla S, McNally A, Husak G and Funk C. 2014. A seasonal agricultural drought forecast system for food-insecure regions of East Africa. *Hydrology and Earth System Sciences*, 18(10): 3907-3921. DOI: 10.5194/hess-18-3907-2014.
- Some'e BS, Ezani A, Tabari H. 2012. Spatiotemporal trends and change point of precipitation in Iran. *Atmospheric research*. 1;113:1-2. DOI: 10.1016/j.atmosres.2012.04.016.
- Tabari H, Talaee PH. 2011. Temporal variability of precipitation over Iran: 1966–2005. *Journal of Hydrology*.13;396(3-4):313-20. DOI: 10.1016/j.jhydrol.2010.11.034.
- Toté C, Patricio D, Boogaard H, van der Wijngaart R, Tarnavsky E and Funk C. 2015. Evaluation of satellite rainfall estimates for drought and flood monitoring in Mozambique. *Remote Sensing*, 7(2): 1758-1776. DOI: 10.3390/rs70201758.

## Tables

*Table 1. Pairwise and categorical statistics (adapted from Toté et al., 2015).  $G$  and  $S$  denote gauge and satellite data, respectively;  $A$  is the number of hits (precipitation detected by both satellite product and at the gauge) and  $B$  is the number of false alarms (precipitation detected by the satellite product but not observed at the gauge).*

Name	Formula	Perfect Score
Pearson Correlation Coefficient	$r = \frac{\sum (G - \bar{G})(S - \bar{S})}{\sum \sqrt{(G - \bar{G})^2} \sqrt{(S - \bar{S})^2}}$	1
Relative Mean Absolute Error (RMAE)	$RMAE = \left( \frac{1}{N} \sum  S - G  \right) / (\bar{G})$	0
Bias	$Bias = \frac{\sum S}{\sum G}$	1
False Alarm Ratio (FAR)	$FAR = B / (A + B)$	0

*Table 2. Validation statistics for all seasons averaged across Iran and over the 2005-2014-time period. Values closest to the perfect score (see Table 1) are underlined.*

Season	Spring	Summer	Autumn	Winter
<b>Correlation</b>	<u>0.621</u>	0.559	0.585	0.453
<b>RMAE</b>	<u>0.66</u>	0.85	0.68	0.88
<b>Bias</b>	1.28	<u>0.90</u>	<u>0.91</u>	1.46
<b>FAR</b>	<u>0.09</u>	0.45	0.28	<u>0.065</u>
<b>Mean Precipitation [mm]</b>	89.53	25.31	89.27	112.50

**Figures**

fig1

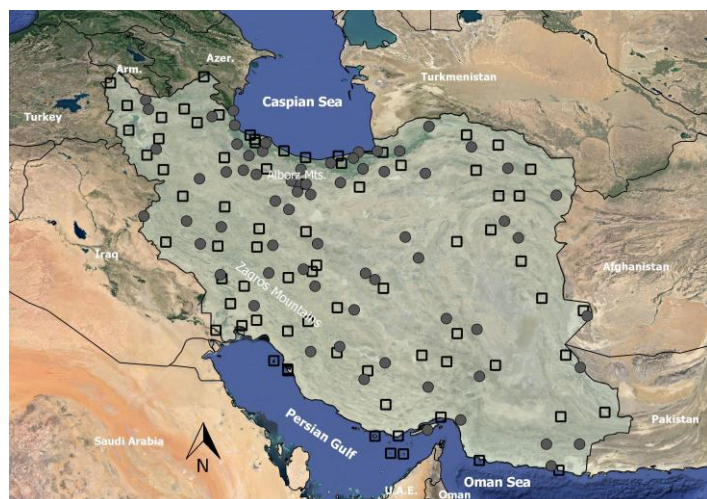


fig2

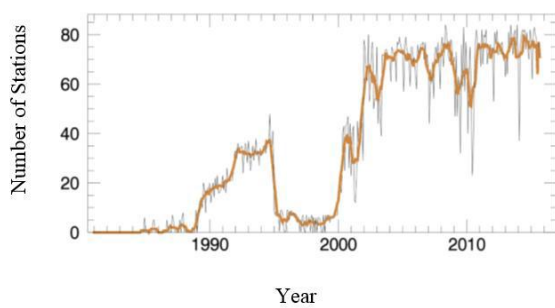


fig3

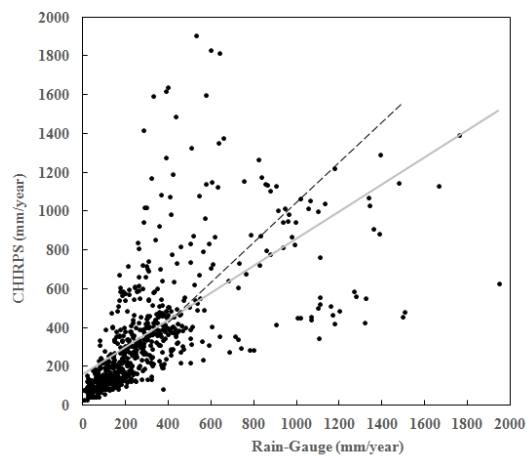


fig4

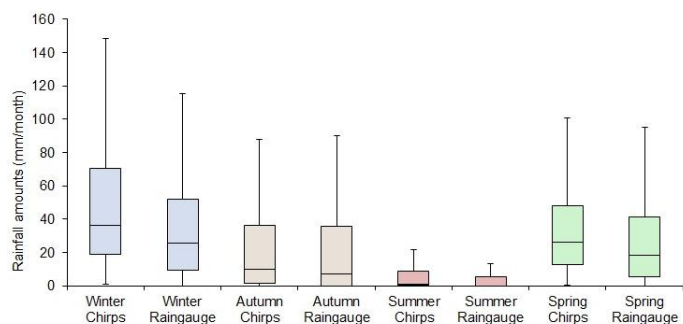
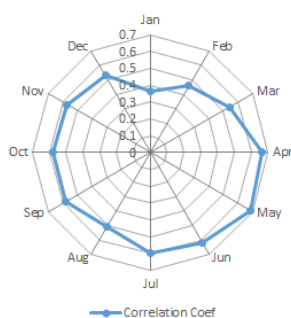
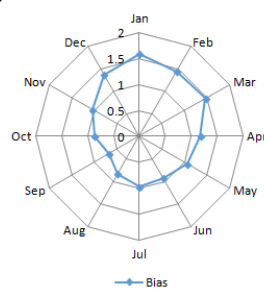


Fig5

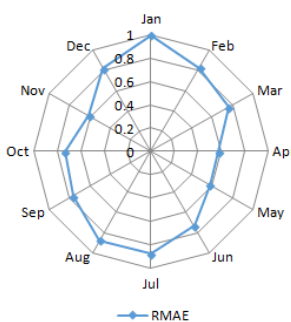
a)



b)



c)



d)

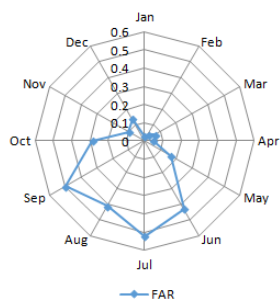




Fig6

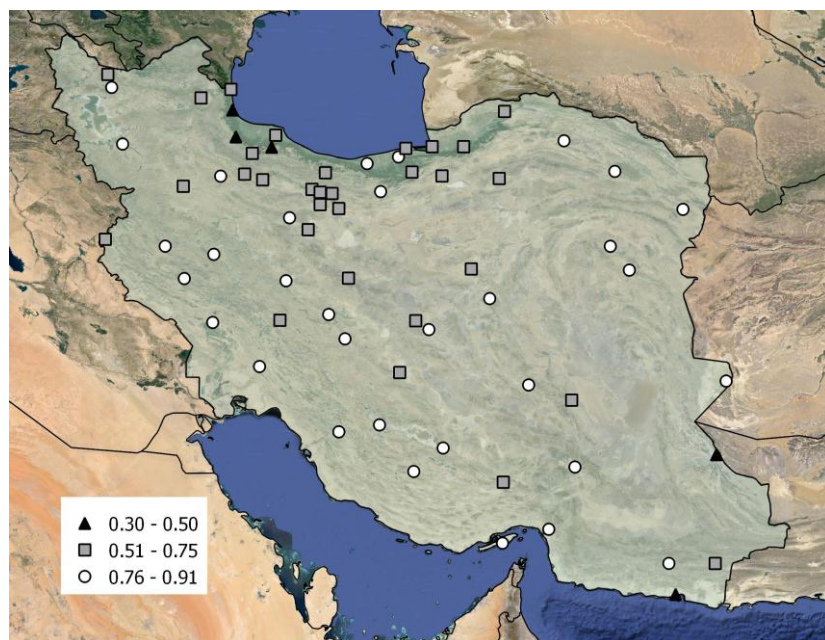


Fig7

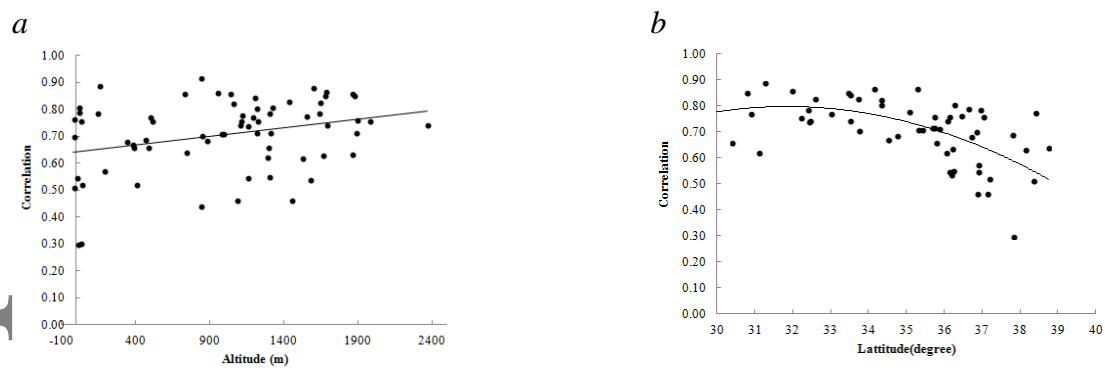


Fig8

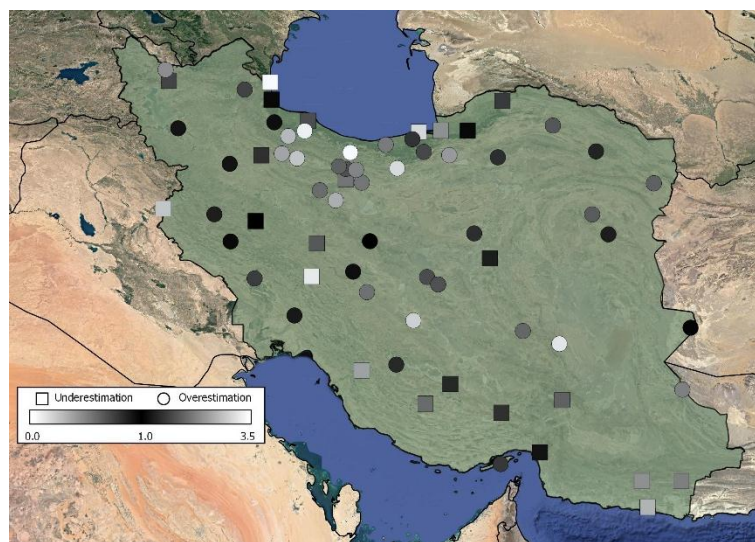


Fig9

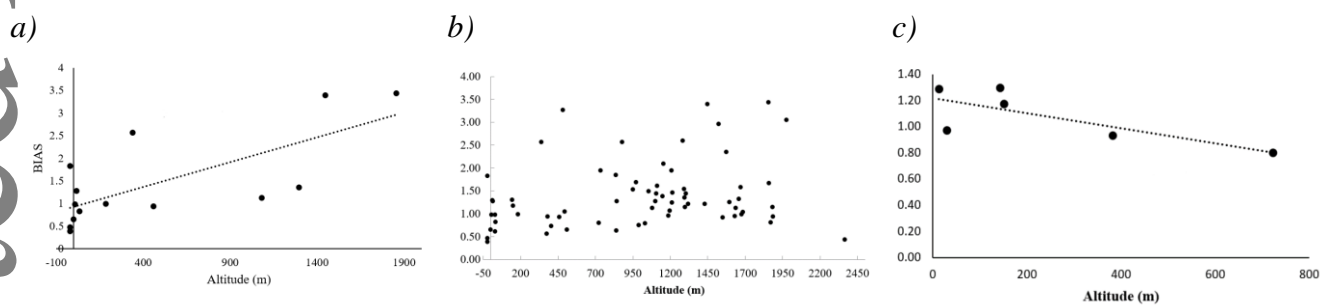


fig10

